

Novel thin film solar cell model with two antipolar MIS structures

D. König, G. Ebest

Department of Electronic Components, Technical University of Chemnitz,
09107 Chemnitz, Germany, *e-mail: dko@infotech.tu-chemnitz.de*

Abstract

In this article we introduce a new thin film solar cell model which uses the properties of two antipolar MIS structures. The active layer consists of unipolar polycrystalline silicon. We employed silicon dioxide as insulator. The back- and top electrode consist of indium tin oxide (ITO). The solar cell model was developed under consideration of the low-temperature chemical vapour deposition (i.e. PECVD). As oxide and ITO are optical transparent medias and in compound with the planned process technology the solar cell concept would be very suitable for a stack arrangement which would increase the device conversion efficiency.

Currently the preparation of silicon dioxide with a sufficiently large fixed negative charge seems to be out of technological facilities. Nevertheless we consider the concept introduced herein as an important contribution to novel ways of efficient low-cost thin film solar cells.

1. Introduction

At present the only type of solar cells in existence using a unipolar active layer is the MIS cell, using an active layer made of single crystalline silicon. Although the efficiency of MIS cells is high they require much energy and time in processing what makes the manufacture somewhat expensive. Poly silicon devices on the other hand require less energy in the manufacturing process but consist of a p-n or p-i-n structure. This structure still can be circumvented by a unipolar thin polycrystalline silicon layer which would save production costs in counts of energy, high-grade silicon and process steps.

This work introduces a new thin film solar cell model which works with a p⁻-doped unipolar thin film of polycrystalline silicon. In contrast to bipolar polycrystalline silicon layers with a p/n or p/i/n structure for load carrier separation the solar cell model introduced herein is realized by two different oxide layers which are put on the polycrystalline silicon layer at the top and bottom surface. For that reason we call this solar cell model the oxide-semiconductor-oxide solar cell (OSOSC). With the planned technologies for putting the solar cell model into practice there exists a good facility to manufacture stacked arrangements.

In the following section the physical shape for the OSOSC is represented. Section 3 shows the working principle of the solar cell. Simulation results are represented in section 4. A conclusion is drawn in section 5.

2. Physical Shape of the OSOSC

Fig. 1 shows the cross-section of the OSOSC.

On a substrate (e.g. glass or stainless steel) a transparent ITO layer with a thickness of 100 nm is deposited. It acts as an optical transparent back electrode. Then an oxide layer (OX1) with a thickness of several 100 nm and a fixed oxide charge per unit area of $|Q_{OX1} = -1 \times 10^{13} \text{ cm}^{-2}$ is put upon the ITO. Subsequently a contact hole is etched through the oxide layer OX1 and filled up with p⁻-doped silicon, $N_A = 1 \times 10^{14} \text{ cm}^{-3}$. As next step the active polycrystalline silicon layer is deposited upon OX1. The polycrystalline silicon layer contains the same doping type and density as the contact hole and has a thickness ranging from 200 nm up to 1 μm . It was found to be optimal for optical reasons at a thickness of 460 nm. For minimizing the grain boundary recombination losses the texture of the polycrystalline silicon layer consists only of vertical grain boundaries. Furthermore the grain boundaries are passivated this way that their surface charge density does not exceed $1 \cdot 10^{11} \text{ cm}^{-2}$. On top of the silicon layer another SiO₂ sheet (OX2) with a fixed oxide charge density per unit area of $|Q_{OX2} = 1 \times 10^{13} \text{ cm}^{-2}$ and a thickness ranging from 200 nm up to 1 μm is deposited. This process is followed by an etching process in order to create a hole in the oxide layer which will inhabit a contact bridge. That hole is filled up with silicon of the same doping type and doping density as the silicon layer. Another ITO layer is deposited then onto the oxide sheet, connecting the different contact bridges and working as an optical transparent top electrode. It has a thickness of 100 nm.

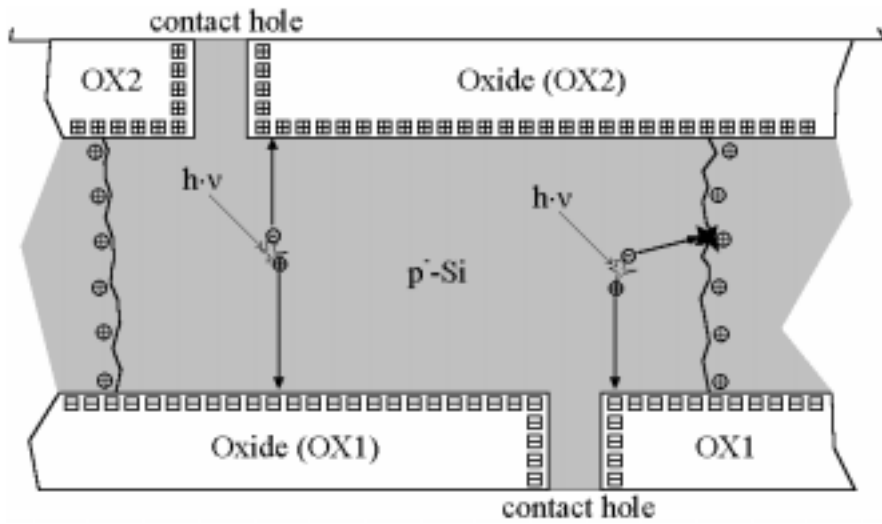


Fig. 1: Physical Shape of the OSOSC.

It has to be stated however that this process sequence was not carried out in practice yet so that it is merely an idea how to put that OSOSC into practice.

3. Working Principle

The OSOSC arrangement combines two antipolar MIS effects for load carrier separation.

The top ITO layer, followed by the oxide layer OX2 and the silicon grain represents an MIS structure. Below the polycrystalline silicon layer a second MIS structure exists (ITO, OX1, silicon). The basic difference to conventional MIS structures lies in the contact of the silicon grain from the ITO layers with help of the contact holes.

As the upper oxide sheet OX2 contains a high density of fixed positive charges there is a high boundary charge. This fixed boundary charge causes a very strong negative band tilting towards the oxide layer OX2. For that reason a very strong drift field exists which concentrates free electrons underneath the OX2 layer, thereby generating an n-inversion layer. Holes are pushed away by the OX2 drift field towards the opposite side of the silicon layer.

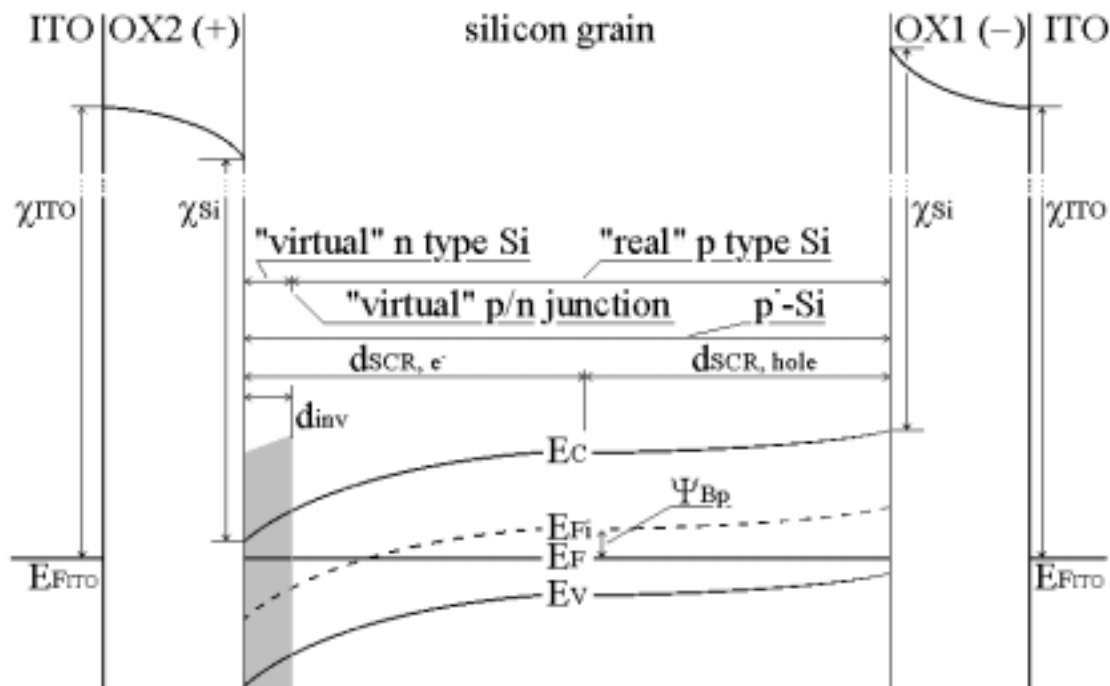


Fig. 2: Energy band diagram of the OSOSC model along a vertical axis; the bottom of the structure is situated at the right side.

The bottom MIS structure acts the opposite way as the oxide layer OX1 contains a high negative fixed charge which concentrates holes at the OX1 layer, thereby creating a hole accumulation layer. Correspondingly electrons are pushed away from the OX1 layer towards the OX2 layer. In this way there exists a unidirectional band tilting which is very suitable for load carrier separation within the whole silicon layer as figure 2 shows.

3. Simulation Results

The simulation was carried out by the simulator ToSCA 3.2 under SUN-OS 5.5.1 on a SUN-SPARC 20 [1]. ToSCA 3.2 is strongly based on [2]. Because of the complexity of the model only one grain of the polycrystalline silicon layer was used as the simulation domain. The simulated structure with computation grid shows Fig. 3.

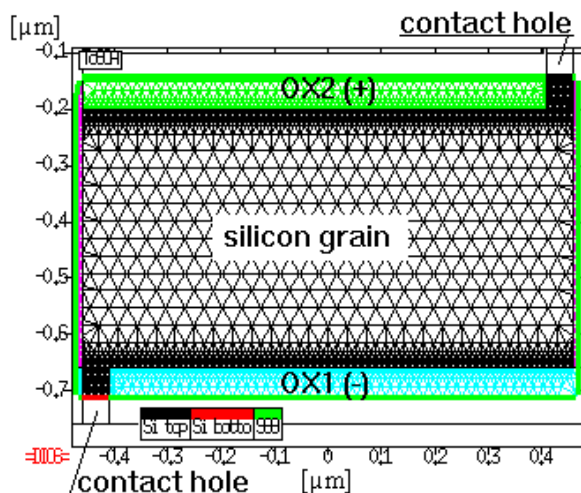


Fig. 3: Simulation structure of the OSOSC (1-grain-model).

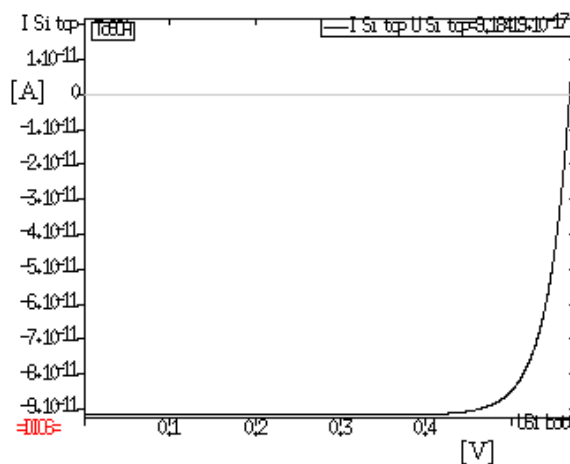


Fig. 4.: Active V-I graph of the 1-grain-model under 1 sun illumination, AM1 conditions.

Unfortunately it does not simulate any tunneling effects nor any alternatively chargeable trap states at grain boundaries. While the tunneling effect plays an important role at the contact of the n-inversion layer the alternatively chargeable traps may hamper the electron current flow over vertical grain boundaries within the n-inversion layer towards the next contact hole.

The maximum power point (MPP) is the most important operation point of a solar cell. For reasons of limited space we represent graphical data of the MPP only.

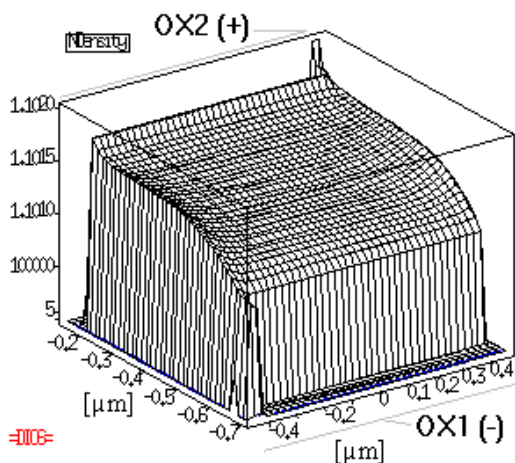


Fig. 5: Electron density within the silicon grain, model works at MPP.

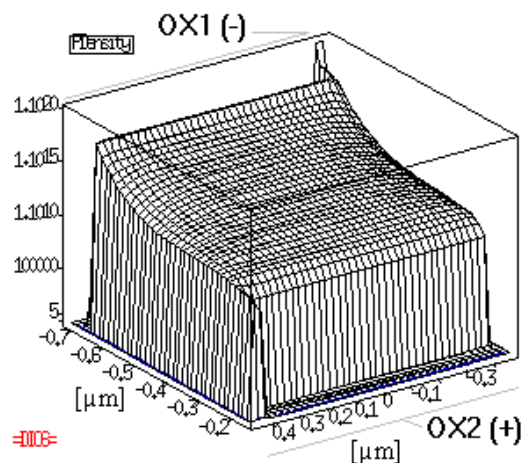


Fig. 6: Hole density of the 1-grain-model working at MPP.

The figures 5 and 6 show the electron and hole density respectively within the simulation domain. As a result of the corresponding band tilting of the relevant MIS structures there exists a strong gradient of both electrons and

holes. Those gradients shape the surface plot of the field strength as seen in figure 7. The peak-like maximas are caused by the corresponding oxide charge and the n-inversion layer/hole accumulation layer.

In figure 8 the vector plot of the field strength reveals the disturbing influence of the grain boundary charges which were assumed to be positive (see sect. 1). Depending on the position of the quasi-Fermi levels those positively charged traps can act as recombination centers. This phenomenon has also an influence on the load carrier transport over several grain boundaries towards the next contact hole.

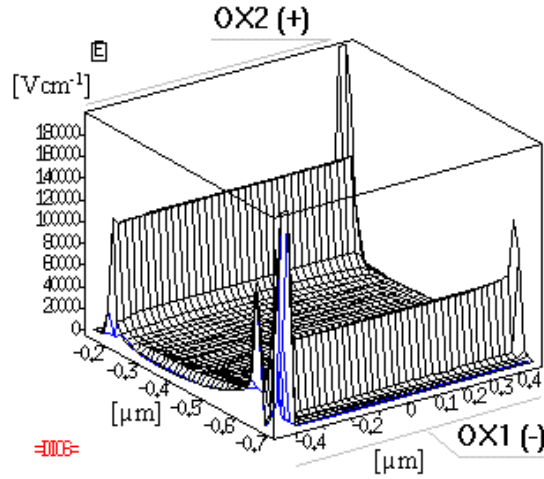


Fig. 7: Typical distribution of field strength over the 1-grain-model, cell works at MPP.

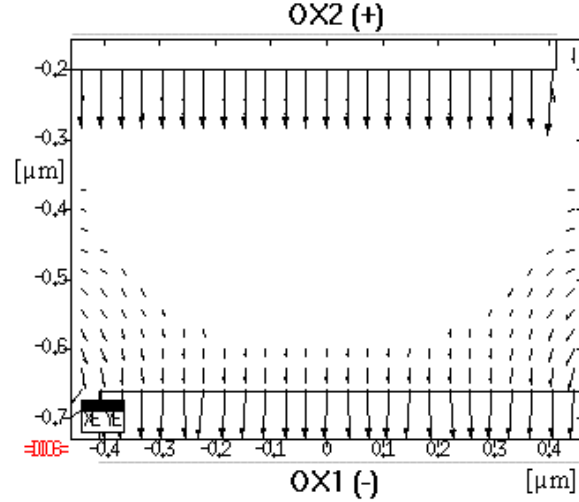


Fig. 8: Vector plot of the field strength within the silicon grain, cell works at MPP; the charge of vertical grain boundaries cause a disturbing field (horizontal component of field vectors).

By integrating the field strength we obtain the surface plot of the potential within the simulation domain as shown in figure 9. Table 1 shows the external simulation results of the 1-grain model.

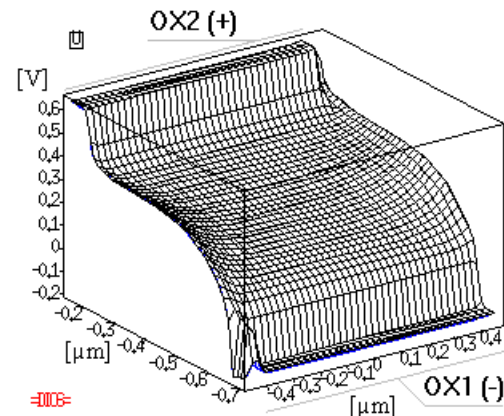


Fig. 9: Potential distribution over the 1-grain model, cell works at MPP.

magnitude	value	magnitude	value
VOC	567 mV	FF	82.0 %
VMPP	510 mV	efficiency	10.3 %
IMPP	9.15 nA	jMPP	9.86 mAcm ⁻²
ISC	8.35 nA	jSC	10.81 mAcm ⁻²

Table 1: Output values of the 1-grain model; the efficiency refers to the *absorbed* photon flux within the active layer.

The optimal thickness of the active layer was estimated to 460 nm, resulting in an photon absorption rate of 48.7 % of the total impinging photon flux. If the *absorbed* photon flux is taken as total input power the conversion efficiency is 10.3 %. If the efficiency is considered against the total photon flux it is reduced to approximately 5.02 %.

By extending the thickness of the active polycrystalline layer to a few microns the absorption rate can reach values close to 100%, thereby increasing total conversion efficiency to 10%. Unfortunately a simulation with a high resolution computation grid of an active layer of say about 5 microns is not possible with the simulation tool

ToSCA3.2 because the workspace memory is limited by the simulator . Nevertheless it is possible to extend the active layer up to a few microns as long as the oxid charges are at least $|Q_{OX2} = -|Q_{OX1} = 1 \times 10^{13} \text{ cm}^{-2}$

4. Conclusion

A new model of a thin film solar cell based upon a unipolar, homogenously doped polycrystalline silicon layer in compound with two antipolar MIS structures was introduced in this study.

The planned CVD technology for putting this solar cell model into practice provides good conditions for a stacked arrangement of several oxide-semiconductor-oxide solar cells (OSOSCs). Other advantages of the CVD technology are its low process temperature and the relatively high process speed.

With the one-grain model an electrical conversion efficiency of 10.3 % was reached. As the theoretical model could not be implemented completely into the Simulator ToSCA 3.2 the results represented are merely a glimpse on the capability of the OSOSC.

We stated that the OSOSC model introduced in this article could represent a reasonable alternative to current solar cell models.

Acknowledgements

The author would like to thank U. Todt and A. Erlebach from the Fraunhoferinstitut for Microelectronics Dresden, Germany, for their selfless support concerning the simulation package DIOS/ToSCA 3.2 .

References

- [1] H. Gajewski et al.: ToSCA (Two Dimensional Semi-Conductor Analysis Package), manual (specified for ToSCA in compound with DIOS), specification: U. Todt, 1993 .
- [2] S. Selberherr: Analysis and Simulation of Semiconductor Devices, Springer Press, Wien/New York, 1984